PCCP

Accepted Manuscript

ROYAL SOCIETY OF CHEMISTRY

www.rsc.org/pccp

Initial Hydration Behavior of Sodium iodide dimer: Photoelectron spectroscopy and *ab initio* calculations

Ren-Zhong Li,[1,2,4] Gao-Lei Hou[2], Cheng-Wen Liu,[3] Hong-Guang Xu[2], Xiang Zhao[4]*, Yi Qin Gao,[3]* Wei-Jun Zheng[2]*

[1]*College of Electronics and Information, Xi'an Polytechnic University, Xi'an 710048, China*

[2]*Beijing National Laboratory for Molecular Sciences, State Key Laboratory of Molecular Reaction Dynamics, Institute of Chemistry, Chinese Academy of Sciences, Beijing 100190, China*

[3]*Beijing National Laboratory for Molecular Sciences, Institute of Theoretical and Computational Chemistry, College of Chemistry and Molecular Engineering, Peking University, Beijing 100871, China*

[4]*Institute for Chemical Physics, School of Science, Xi'an Jiaotong University, Xi'an 710049, China*

**Corresponding author. Email: xzhao@mail.xjtu.edu.cn, gaoyq@pku.edu.cn, zhengwj@iccas.ac.cn,*

Tel: +86 10 62635054, Fax: +86 10 62563167

Abstract

We investigated $(NaI)_2^-(H_2O)_n$ (n = 0-6) clusters to examine the initial solvation process of $(NaI)_2$ in water, using negative ion photoelectron spectroscopy and theoretical calculations. The structures of these clusters and their neutrals were determined by comparing the *ab initio* calculations with the experiments. It is found that the bare $(NaI)_2^-$ is a L-shaped structure and the corresponding neutral is a rhombus. In $(NaI)_2^-(H_2O)$, the water molecule prefers to interact with the middle Na atom of the L-shaped $(NaI)_2^-$. For $(NaI)_2^-(H_2O)_n$ clusters with n = 2-3, two types of structures are nearly degenerate in energy: one is L-shaped and the other is pyramid-shaped. As for $(NaI)_2^-(H_2O)_n$ with n = 4-6, the dominant structures are pyramid-shaped. For the anionic clusters, one of the Na-I distances increase abruptly when n equals 2; for the neutral clusters, the rapid lengthening of the Na-I distances occurs at n = 4. Additionally, the analyses of the reduced density gradient were carried out, and the results reveal that the Na^+-water interactions dominate in $(NaI)_2^-(H_2O)_n$ for $n \leq 4$, whereas the I^--water and water-water interactions are significantly enhanced when n increases to 5.

1. Introduction

Investigate the interactions between alkali-halide clusters and water molecules can give insights into the dissociation and dissolution processes of salts. The studies can provide useful information for atmospheric and environmental chemistry,[1-3] as the dissolution of sea salt particles plays an important role in producing halogen anions, which can destroy ozone (a key species in the atmospheric chemistry) via photochemical processes.[4] Although salt-water clusters have been investigated previously by both experiments[5-9] and theory,[10-20] the interactions between water and alkali-halide in the gas phase, especially, the interactions of water molecules with clusters containing multiple alkali-halide units, have not been studied in details by experiments.

As for the hydration of sodium iodine, the monomer has been investigated by many groups, because of its importance in photodissociation dynamics.[21-24] Olleta et al. studied the structures, binding energies, electronic properties of $NaI(H_2O)_{1-6}$ based on *ab initio* calculations, and found that pentahydrated and hexahydrated clusters show dissociated structures.[25] Peslherbe and co-workers[23-24, 26-27] investigated the structures, dynamics and stability of NaI-water systems using molecular dynamics simulations and found that the ion pair is quite stable with respect to dissociation into free ions, even in large clusters. Grigoire et al.[28-30] studied the $NaI-(H_2O)_n$ and $NaI-(NH_3)_n$ clusters by performing resonance-enhanced two-photon ionization experiments. Their results show that a solvent-selective ionization behavior for sodium iodide clustered with various solvents. Raymond et al.[31] studied the molecular structure and bonding of the surface of salt solutions of NaX (X: F, Cl, Br, I) using vibrational sum-frequency spectroscopy and the results indicated that the population of the anions at the uppermost layer of the surface diminished significantly. In addition, there also exist studies on the hydration of alkali-rich sodium iodide. Blades et al.[32] studied the hydration energies of $(MI)_mM^+$ ions in the gas phase, where $M^+ = Na^+$, K^+, Rb^+, Cs^+, with up to four water molecules, and their study show that the sequential hydration bond energies for $MIM(H_2O)_n^+$ and $(MI_m)M^+$ decrease with increasing n and m, respectively. Zhang et al.[33] studied the dissolution processes of Na_2I^+ and $Na_3I_2^+$ with the association of water molecules, and found that the separation of the Na-I ion pair for Na_2I^+ occurs when six H_2O molecules are added to the salt cluster and only one or two H_2O molecules are added to the salt cluster for $Na_3I_2^+$. Only a limited number of studies on the hydrated clusters containing more than one alkali-halide units have been conducted. Woon[34] studied $(LiF)_2$ and $(LiF)_2(H_2O)$ based on MP2 calculations, and suggested that the water causes a large distortion of the nearest LiF

bond, with a change in $(LiF)_2(H_2O)$ almost twice as large as in $LiF(H_2O)$. Liu et al.[35] studied the $(NaCl)_3(H_2O)_n$(n = 2-7) and found that the water molecule preferentially binds to the Na-Cl edge. Yamabe et al.[16] studied the mechanism of the ion separation of the NaCl microcrystal via the association of water with $(NaCl)_m$. Fatemi and Bloomfield[36] studied the $(NaI)_nH_2O^-$(n = 3, 4, 6) using photoelectron spectroscopy and found that the water molecule attaches to the edge of NaI particle and orients itself to decrease NaI particle's electron affinity.

In this work, in order to get a better understanding of how alkali-halide clusters interact with water molecules, we conducted a combined experimental/theoretical study of the initial solvation process of $(NaI)_2$ in water by negative ion photoelectron spectroscopy of $(NaI)_2^-(H_2O)_n$ (n = 0-6) clusters and *ab initio* calculations.

2. Experimental and Theoretical Methods

2.1 Experimental Methods

The experiments were conducted on a home-built apparatus consisting of a time-of-flight (TOF) mass spectrometer and a magnetic-bottle photoelectron spectrometer, which has been described previously.[37] Various sodium iodide clusters containing water molecules were produced in a laser vaporization source and then analyzed using the TOF mass spectrometer. In the experiment, a rotating and translating NaI disk target was ablated by the second harmonic (532 nm) light pulses from a Nd:YAG laser, while helium carrier gas with ~4 atm backing pressure seeded with water vapor was allowed to expand through a pulsed valve to generate and cool the hydrated sodium iodide clusters. The $(NaI)_2^-(H_2O)_n$ (n = 0-6) clusters were each mass-selected and decelerated before being photodetached by the 532 nm photons from another Nd:YAG laser. The photodetached electrons were energy-analyzed by the magnetic-bottle photoelectron spectrometer. The photoelectron spectra were calibrated with the spectra of Cs^- and Bi^- taken at similar conditions. The instrumental resolution was approximately 40 meV for electrons with 1 eV kinetic energy.

2.2 Theoretical Methods

The theoretical calculations were performed using GAUSSIAN 09 program package.[38] The structures of $(NaI)_2^-(H_2O)_n$ and their neutrals were fully optimized with density functional theory (DFT) employing the long-range correction in combination with the short-range variant of the Perdew-Burke-Ernzerhof (PBE) exchange functional LC-ωPBE,[39-41] which has been previously shown to be suitable to study the salts-water

clusters.[42] The Pople's all-electron basis set 6-311++G(d, p)[43] was used for the Na, O, and H atoms. The effective core potential (ECP) basis set LANL2DZdp,[44] as obtained from the EMSL basis set library,[45] was used for I atoms. The initial structures of $(NaI)_2^-(H_2O)_{1-3}$ clusters were obtained by varying the positions of the water molecules. The large clusters (n>3) were generated by adding water molecules to the different plausible positions of the smaller ones. Frequencies were calculated to verify that the optimized structures correspond to real minima on the potential energy surface. The theoretical vertical detachment energies (VDEs) were calculated as the energy differences between the neutrals and the anions both at the optimized anionic structures. The theoretical adiabatic detachment energies (ADEs) were calculated as the energy differences between the neutrals and the anions with the neutrals relaxed to the nearest local minima using the geometries of the anions as initial structures. We further performed single-point energy calculations at high-level ab-initio CCSD(T) (couple-cluster with single and double and perturbative triple excitations)[46-47] for $(NaI)_2^{-/0}(H_2O)_{0-4}$ clusters with the same basis set to get more accurate energetic information. All the relative energies and theoretical ADEs have been corrected by the zero-point vibrational energies (ZPEs) obtained at the LC-ωPBE/6-311++G(d, p) level of theory. To evaluate the uncertainty of DFT method, the structures of $(NaI)_2^-(H_2O)_{1-3}$ clusters were also optimized using MP2[48-50] method, which gave essentially the same results as LC-ωPBE method (see Supplementary Materials). Additionally, a visual study of cation−anion, cation−water, anion−water, and water−water interactions were performed by calculating the reduced density gradient (RDG) proposed by Yang group,[51] based on the electron density ($\rho(r)$) and its first derivative ($s = 1/(2(3\pi^2)^{1/3}) |\nabla\rho|/\rho^{4/3}$) and the second largest eigenvalue (λ_2) of Hessian matrix of electron density functions, by using the Multiwfn program.[52] The RDG can be used to describe the deviation from a homogeneous electron distribution within density functional theory. As a fundamental dimensionless variable, the reduced gradient is found to be the ratio of density and gradient values and the noncovalent interactions can be clearly isolated in real space. The regions of noncovalent interactions marked with the gradient approach zero and equal zero at the critical point. The different noncovalent interaction types can be distinguished by the values of $sign(\lambda_2)(\rho)$.[51] Thus, the RDG can be used to analysis noncovalent interactions in cluster systems.

3. Experimental Results

The photoelectron spectra of $(NaI)_2^-(H_2O)_n$ (n = 0-6) clusters measured with 532 nm photons are shown in Figure 1. The VDEs and ADEs of these clusters estimated from their

spectra are summarized in Table 1.

The photoelectron spectrum of bare $(NaI)_2^-$ at 532 nm shows an unresolved broad band feature centered at about 1.70 eV. The ADE of $(NaI)_2^-$ is estimated to be 1.56 ± 0.08 eV. The spectrum has a large change with a new band X′ showing up at the lower binding energy side when the first water molecule adsorbed on $(NaI)_2^-$. The measured spectrum in the experiment shows that the major band feature X has a VDE of 1.62 eV and the weak new band X′ has a lower VDE of 1.24 eV. Similar to $(NaI)_2^-(H_2O)$, the double-peak spectral pattern in the threshold region are also observed in the spectra of $(NaI)_2^-(H_2O)_n$ (n = 2-3), except that the peaks shift to lower binding energy and the relative intensities of the X′ versus X band when n increases from 1 to 3. The peaks (X′ and X) of $(NaI)_2^-(H_2O)_2$ are centered at ~1.18 and 1.62 eV, respectively, and those of $(NaI)_2^-(H_2O)_3$ are centered at ~1.04 and 1.59 eV, respectively. These observations indicate that two kinds of isomers may coexist in the spectra of $(NaI)_2^-(H_2O)_n$ (n = 1-3), corresponding to the X′ and X spectral features. The photoelectron spectra of $(NaI)_2^-(H_2O)_n$ with n = 4-6 each have only a major broad feature X′, and the band X at higher binding energy side disappears, suggesting that there is only one kind of dominating structure. The VDE of $(NaI)_2^-(H_2O)_4$ is measured to be about 1.00 eV, those of $(NaI)_2^-(H_2O)_5$ and $(NaI)_2^-(H_2O)_6$ shift to higher electron binding energies of 1.07 and 1.08 eV, respectively.

The change of VDEs with the number of water molecules in $(NaI)_2^-(H_2O)_n$ (n = 0-6) clusters are shown in Figure 2. It can be seen that the VDEs of X of $(NaI)_2^-(H_2O)_n$ first decreases when n changes from 0 to 1, stays nearly unchanged from 1 to 2, and then decreases again as n increases to 3. As for the VDE of X′ of $(NaI)_2^-(H_2O)_n$, the value first decreases when n changes from 1 to 4, and then increases when n increase from 4 to 6. These observations suggest that the Na-water interaction are very strong for $(NaI)_2^-(H_2O)_n$ from n = 0 to 4, and the I^--water and water-water interactions are dominating when the fifth and sixth water adsorbing, as it has been analyzed previously that the alkali metal-water interactions reduce the VDEs while the anion-water and water-water interactions increase the VDEs.[42] These inferences will be confirmed by the analysis of interactions in Section 4.

4. Theoretical Results and Discussion

4.1 The structures of $(NaI)_2^-(H_2O)_n$ and $(NaI)_2(H_2O)_n$ (n = 0 - 6)

The optimized structures of the typical low-lying isomers of $(NaI)_2^-(H_2O)_n$ are presented in Figures 3 and 4, while the neutral structures are shown in Figures 5 and 6. The theoretical relative energies and VDEs of these low-lying isomers are listed in Table 2 and compared

with the experimental values.

Our calculations show that the global minimum of $(NaI)_2^-$ is 0A in ^2A state with a L-shaped structure and C_s symmetry, and the angle ∠Na-I-Na is 122.5°. The theoretical VDE of $(NaI)_2^-$ is 1.62 eV with CCSD(T) method, close to the experimental value of 1.70 eV measured in this work. Isomer 0B is higher than 0A by 0.27 eV and it is a ring structure with C_{2v} symmetry and $^2A_1$ state. The calculated VDE of 0B is 0.62 eV, largely deviating from the experiment measurement. Therefore, we conclude that the L-shaped structure makes a main contribution to the photoelectron spectrum. For $(NaI)_2$ neutral, the most stable structure 0A′ is a rhombus with C_{2v} symmetry, different from the square structure suggested by previous theoretical calculations.[53] The significant deformation between the most stable structures of $(NaI)_2^-$ and the corresponding neutral one indicates that the excess electron has induced a significant change to the $(NaI)_2$ framework.

We can see that the typical minimal energy structures of $(NaI)_2^-(H_2O)$ are formed by attaching a water molecule to the L-shaped $(NaI)_2^-$. In the most stable structure 1A, the water molecule interacts with the nearest Na1-I1 unit with its oxygen atom connecting to the middle Na atom (Na1) and with one H atom pointing to the terminal I atom (I1), and the Na1-I1 distance is longer than that in bare $(NaI)_2^-$ by 0.12 Å. The theoretical VDE of 1.77 eV is in agreement with the experimental VDE (1.62 eV) of the second peak (X) in the photoelectron spectrum of $(NaI)_2^-(H_2O)$. In isomer 1A, the Na1-O bond length of 2.32 Å is shorter than I1-H length of 2.72 Å, indicating that the Na-water interaction is stronger than I-water interaction. This observation indicates that the negative end of permanent dipole of water molecules prefer to pointing toward the Na1-I1 portion of $(NaI)_2^-(H_2O)$ and weaken the electron's attachment. Such a result is consistent with the spectrum of $(NaI)_2^-(H_2O)$ being shifted to a lower binding energy compared with that of bare $(NaI)_2^-$. A similar result can be found in the previous work of $(NaI)_n^-(H_2O)$ (n = 3, 4, 6) by Fatemi and Bloomfield.[36] They reported that the water could orient itself to decrease the electron affinity of alkali-halide. In isomer 1B, the water molecule interacts with the terminal Na atom (Na2) via its O atom and has one of its H atom forming a hydrogen bond with I2. The water does not significantly distort the bare $(NaI)_2^-$, except that the Na2-I2 distance is increased by only 0.29 Å. The calculated VDE of 1B at CCSD(T) level is 1.37 eV, close to the measurement of the VDE(X′) of 1.24 eV in our experiment. So the weak band X′ is most likely due to the contribution from isomer 1B. The most stable isomer of neutral $(NaI)_2(H_2O)$ can be considered as derived from 0A′, with an extra water molecule added via Na-O and I-H interactions.

For $(NaI)_2^-(H_2O)_2$, 2A, 2B and 2C are almost degenerate in energy. In isomer 2A, the

$(NaI)_2^-$ unit remains a L framework with two water molecules inserting between Na1 and I1. It is noteworthy that the distance between Na1 and I1 abruptly increases to 4.59 Å, significantly longer than that in bare $(NaI)_2^-$. The theoretical VDE of 2A calculated with CCSD(T) method is 1.65 eV, in good agreement with the experimental VDE of the higher binding energy peak of 1.62 eV. In isomer 2B, $(NaI)_2^-$ forms a pyramid-shaped unit with Na2 sits at the apex site. The distances between Na2 and two adjacent O atoms are 2.39 Å, shorter than those between Na1 and O atoms (2.53 Å), I1 or I2 and its adjacent H atoms (2.49 Å). This result thus suggests that the Na2-O interaction is dominant in isomer 2B. The distances between Na2 and the two I atoms are elongated to 5.12 Å, indicating that Na2 atom would leave the $(NaI)_2^-$ unit. The theoretical VDE of isomer 2B with CCSD(T) is 1.39 eV, close to the VDE of the lower binding peak. Isomer 2C is derived from 1A with the H atom of the second water interacting with I atom and its O atom interacting with Na atom. The calculated VDE of 2C is 1.13 eV with CCSD(T) method, consistent with the experimental value of 1.18 eV of the first peak X′. Thus it is likely that both isomers 2B and 2C make contributions to the first peak at lower binding energy and 2A contributes to the second peak at higher binding energy. From Figure S1, the relative energies between 2A and 2B changed slightly for the LC-ωPBE and MP2 methods. But the changes of the relative energies are under the uncertainties of theoretical calculations. Thus both the LC-ωPBE and MP2 methods give reasonable results. From Figure 5, we can see that all neutral isomers are derived from 1A′. 2A′ and 2B′ are degenerate, and 2C′ is higher than the global minimum by 0.08 eV in energy. Isomer 2A′ has a C_{2v} symmetry, the second water interacts with another Na atom via its O atom and connects to the same I atom that interacting with the first water, 2B′ with C_{2h} symmetry has a similar structure except one water prefers to form a hydrogen bond with the other I atom. In 2C′, the two water molecules interact with the same Na atom.

For $(NaI)_2^-(H_2O)_3$, three low-lying isomers nearly degenerate in energy are found, as presented in Figure 3. Isomer 3A is derived from 2A with the third water molecule interacting with Na1 atom via its O atom, and interacting with I1 atom via one of its H atoms. The length between Na1 and I1 is 4.36 Å, longer than that of bare $(NaI)_2^-$ by 1.53 Å. The calculated VDE of 3A is 1.50 eV at CCSD(T) level of theory, in good agreement with the experimental VDE(X) of 1.59 eV. So we conclude that isomer 3A yields the VDE of the second peak X at higher binding energy. Isomer 3B is derived from 2B, with the H atom of water interacting with the nearest I atom and the O atoms of water connecting with the adjacent Na atoms and its calculated VDE is 1.04 eV with CCSD(T) method. Isomer 3C is derived from 2C with the additional water sitting between Na1 and I1, the Na1-I1 distance

increases to 4.16 Å. The calculated VDE is 1.10 eV at CCSD(T) level of theory. It is noteworthy that both the calculated VDE of 3B and 3C are both consistent with the experimental VDE(X′, 1.04 eV) of the lower binding energy peak. Therefore we conclude that isomers 3B and 3C make contributions to the lower binding energy peak. Similar to $(NaI)_2^-(H_2O)_2$, the relative energies between 3A and 3B also changed slightly for the LC-ωPBE and MP2 methods, and the change are under the uncertainties of theoretical calculations (Figure S1). As for the neutrals, the most stable isomer 3A′ can be considered as 2A′ attaching the third water to interact with one Na atom via its O atom and to form a hydrogen bond with a I atom via one of its H atoms. Isomer 3B′ has C_s symmetry, is derived from isomer 2A′ with the additional water molecule interacting with one Na atom via its O atom and with the same I atom through one of its H atoms.

For $(NaI)_2^-(H_2O)_4$, the global minimum isomers are shown in Figure 4 and they differ in energy by only 0.08 eV at LC-ωPBE level. Isomers 4A and 4B can be considered as pyramid-shaped structures based on the framework $(NaI)_2^-$. Isomer 4A has a C_s symmetry, each I atom of the $(NaI)_2^-$ unit interacts with three H atoms of three water molecules and the Na atoms interact with the adjacent oxygen atoms. In isomer 4B, there are three H atoms of three water molecules pointing to I1, and two H atoms of two water molecules pointing to I2. The calculated VDEs of 4A and 4B with CCSD(T) method are 1.16 and 1.07 eV, respectively, close to the experimental VDE of 1.00 eV. So we suggest that band feature of experiment are contributed collectively by isomers 4A and 4B. For the neutral isomers, the $(NaI)_2$ unit of the most stable 4A′ has C_{2v} symmetry with four water molecules sitting around one side of the quadrilateral unit $(NaI)_2$. The distances of both Na1…I1 and Na2…I1 abruptly increase to 4.36 Å, whereas the Na1…I2 and Na2…I2 distances are 2.96 Å, only slightly different from those in bare $(NaI)_2$ unit. This indicates that the water molecules' interferences induced a significant change to the $(NaI)_2$ unit. 4B′ is derived from 3A′, just 0.02 eV higher than 4A′, the further calculated energy difference is 0.18 eV with CCSD(T) method, and each Na atom interacts with two water molecules.

For $(NaI)_2^-(H_2O)_5$, two low-lying isomers derived from 4A are found. In the most stable isomer 5A, the fifth water molecule interacts with a Na atom via its O atom and interacts with the adjacent I via one of its H atoms, and with the other H atom pointing to the O atom of the nearest water to form a water-water H-bonding. The VDE of 5A is calculated to be 1.29 eV with LC-ωPBE method. As the experimental photoelectron peak is very broad and extends in the range of 0.76 – 1.47 eV. Thus, isomer 5A may contribute to the high EBE part of the photoelectron peak. Isomer 5B is higher in energy than 5A by only 0.05 eV, with the

additional water molecule interacting with Na2 via its O atom. The calculated VDE of 5B is 1.08 eV with LC-ωPBE method, in agreement with the experimental VDE of 1.07 eV. Considering the calculation error limit, we conclude that both 5A and 5B exist in the experiment. As for the neutral isomer, the most stable isomer 5A' is built by attaching an additional water molecule to 4A' by interacting with Na1 via its O atom and forming a hydrogen bond with I2. For $(NaI)_2^-(H_2O)_6$, two typical low-lying isomers with water-water H-bonds are found. The most stable structure 6A is derived from 5A, and the sixth water molecule interacts with I2 via one H atom and interacts with O atom of the adjacent water to form water-water H-bonding via another H atom. The theoretical VDE of 6A (1.25 eV) calculated at LC-ωPBE level of theory is close to the experimental VDE of 1.08 eV. As for isomer 6B, it can considered as derived from 5B with the additional water interacting with I1 and Na1 via one H atom and O atom respectively. The other H atom of the additional water interacts with the adjacent water to form a water-water H-bond. The calculated VDE of 6B (1.08 eV) is in excellent agreement with the experimental VDE. Therefore, both isomers 6A and 6B make contributions to the spectrum of the experiment. As for the neutrals of $(NaI)_2(H_2O)_6$, two isomers degenerate in energy (6A' and 6B') are found. Isomer 6A' is C_s symmetry structure derived from 5A', with the sixth water molecule sitting between Na2 and I2. The distances between I1 and the two Na atoms are both 4.41 Å, and the Na1-I2 and Na1-I2 distances are both 3.17 Å. In isomer 6B', four water molecules sit around one side of the quadrilateral $(NaI)_2$ unit and the other two water molecules sit between Na1 and I4. The I1-Na2, I1-Na1, I2-Na1 and I2-Na2 distances are 4.28, 4.40, 3.77 and 2.98 Å respectively. From this, we can see that the Na-I distances are significantly affected by the water molecules.

4.2 The ion separation in $(NaI)_2^-(H_2O)_n$ and $(NaI)_2(H_2O)_n$ (n = 0 - 6)

The structures mentioned above and the Na-I distances listed in Tables S1 and S2 (see Supplementary Materials) reflect very interesting properties. For the anion clusters, the distance between the middle Na atom and the terminal I atom in the L-shaped structures and the distances between the Na atom at apex and the two I atoms in the pyramid-shaped structures increase abruptly when the number of water molecules is equal to two. That reveals that the terminal I^- ion is separated from the L-shaped $(NaI)_2^-$ unit, and the apex Na atom is firstly separated from the pyramid-shaped $(NaI)_2^-$ unit. However, for the neutrals, the abrupt elongation of distances between an I atom and the two Na atoms occurs when the number of water molecules increases to 4 (isomer 4A' in Figure 6). It is interesting to note

that it is an I^- ion firstly separated from the neutral $(NaI)_2$ by the water molecules instead of a Na^+ ion.

In order to understand the structural variation mechanism of $(NaI)_2^-(H_2O)_n$ (n = 0-6) anion versus their corresponding neutrals, we carried out natural population analysis (NPA)[54] and calculated NPA charges. The NPA charge distributions (see Supplementary Materials) show that Na2 in neutral $(NaI)_2(H_2O)_n$ is positively charged 0.72 to 0.87 e, whereas the charge of Na2 in the corresponding anion $(NaI)_2^-(H_2O)_n$ is -0.04 to -0.07 e, that is, the charge of Na2 is reduced by 0.72 to 0.91 e while the charges on the other Na and I atoms are almost unchanged, therefore the excess electron of anion $(NaI)_2^-(H_2O)_n$ is mainly localized on Na2. The addition of the excess electron weakens the Coulomb attraction between Na2 and the adjacent I ions compared with that in the corresponding neutral, so the $(NaI)_2^-$ unit can form L-shaped or pyramid-shaped structure rather than a ring like that in neutrals. Na2 atom can be more easily separated from the $(NaI)_2^-$ unit in the pyramid-shaped structures of anion clusters because of the weak interaction between Na2 and the two I atoms.

In addition, from the analysis of the structures, we can see that both in the anionic and the neutral isomers, water molecules prefer to stay near the Na rather than I, and I always stay out the surface, this is similar to $MI(H_2O)_n^-$(M=Li, Cs).[42] Some previous works[8, 17, 28] reported that the polarizable iodide anion is poorly solvated and presents at the surface of the water cluster. Our results are consistent with the previous works.

4.3 Interaction analyses

Figure 7 shows the calculated electron localization function (ELF)[55] of $(NaI)_2^-$. It can be seen that there is nearly no electron pairing density between the Na and I atoms, indicating that the chemical bonds in $(NaI)_2^-$ are mainly ionic instead of covalent.

To investigate and visualize the cation−anion, cation−water, anion−water, and water−water interactions in the $(NaI)_2(H_2O)_n^-$ clusters, we carried out reduced density gradient (RDG) analysis. The reduced density gradient, coming from the density and its first derivative, is a very useful method to explore noncovalent interactions. Figure 8 displays the gradient isosurfaces of the $(NaI)_2(H_2O)_n^-$ (n = 1-6) cluster anions. From Figure 8, we can see that the green areas localize near the terminal Na atom (Na2) in $(NaI)_2^-H_2O_n$ clusters. This indicates that the excess electron of $(NaI)_2^-H_2O_n$ cluster is mainly localized on its terminal Na atom, consistent with the result of the NPA analysis mentioned in the previous section.

As can be seen in Figure 8, for $(NaI)_2H_2O^-$, the regions between Na and I atom as well as that between one H atom of water and the terminal I atom is dominated by light green

color, indicating that there are mainly weak attractive interactions in these regions; while the region between the O atom of water and its adjacent Na atom shows blue color, indicating a strong electrostatic attraction. This is consistent with the results in the previous sections, that is, the bond length of Na-O is shorter than that of I-H. The strong Na^+-water interaction would reduce the VDE of $(NaI)_2H_2O^-$ by stabilizing the product state of photodetachment, the corresponding neutral. This is responsible for the shift of VDE to lower binding energy for $(NaI)_2H_2O^-$compared to that of bare $(NaI)_2^-$.

For $(NaI)_2(H_2O)_n^-$ with n = 2 - 4, the RDG isosurfaces of the L-shaped structures show blue color disks between the middle Na atom and its adjacent O atoms of water, revealing that the Na^+-water interaction are still dominant. Additionally, the regions between the terminal I atom and the neighboring H atoms of water are light blue accompanied with green, indicating the interactions are enhanced compared with those in $(NaI)_2(H_2O)^-$. For the pyramid-shaped structures at n = 2- 4, the isosurfaces between Na atoms and the adjacent O atoms of water show blue color, indicating very strong electrostatic attraction between Na and water; while the regions between I atoms and the adjacent H atoms have light-blue accompanied with green, showing the characteristics of weak H-bonding.

As for the most stable isomers of $(NaI)_2(H_2O)_5^-$ and $(NaI)_2(H_2O)_6^-$, we can see that the interaction regions of two I atoms and their adjacent H atoms are blue accompanied with green and the interaction region of water-water are blue; while the interaction regions of the Na atoms and their neighboring O atoms of water show light green. These results indicate that the I^--water and water-water interactions are considerably enhanced and dominant in $(NaI)_2(H_2O)_5^-$ and $(NaI)_2(H_2O)_6^-$. This may explain why the VDEs of $(NaI)_2H_2O_n^-$ shift toward higher EBE at n=5-6.

5. Conclusions

The VDEs and ADEs of $(NaI)_2^-(H_2O)_n$ (n = 0-6) clusters are determined from the photoelectron spectra, and the most probable structures of each clusters are determined by comparing the theoretical VDEs with the experimental results. It is shown that the bare $(NaI)_2^-$ is a L-shaped structure. The first water molecule prefers to interact with the middle Na atom of the L-shaped $(NaI)_2^-$ unit. Two types of structures are found when two/three water molecules are attached to the salt cluster: one type is derived from L-shaped structure of bare $(NaI)_2^-$ and the other one is considered as pyramid-shaped structure. More interestingly, the L-shaped structures disappear while the pyramid-shaped structures start to be dominant when n is equal or larger than 4. For the anionic clusters, one of the Na-I

distances (the distance between the terminal I atom and the middle Na atom) in the L-shaped structures increases abruptly when n = 2 and the distances between the apex Na atom and the two I atoms in the pyramid-shaped structures also increase abruptly when n = 2. An I^- ion is separated from the L-shaped $(NaI)_2^-$ unit while a Na atom is firstly separated from the pyramid-shaped $(NaI)_2^-$ unit. However, for the neutrals, the distances between one I atom and two Na atoms are elongated abruptly at n = 4 with the I^- ion firstly separated from the $(NaI)_2$ cluster. From the structures and the reduced density gradient (RDG) analyses, it can be found that the Na^+-water interaction are dominant until the number of water increased to four, and then the I^--water and water-water interactions are considerably enhanced.

ACKNOWLEDGEMENTS. WJZ and YQG acknowledge the Beijing National Laboratory for Molecular Sciences for financial support. RZL thank the National Natural Science Foundation of China (NSFC, Grant No.21301134), Open Fund of Beijing National Laboratory for Molecular Sciences (No. 2013003) for support, Scientific Research Program Funded by Shanxi Provincial Education Department (No. 2013JK0655) and Postdoctoral Science Foundation of China (No. 2015M572545). Part of the theoretical calculations were conducted on the ScGrid and DeepComp 7000 of the Supercomputing Center, Computer Network Information Center of Chinese Academy of Sciences.

REFERENCES

1 K. W. Oum, M. J. Lakin, D. O. DeHaan, T. Brauers and B. J. Finlayson-Pitts, *Science* 1998, **279**, 74.

2 F. Schweitzer, L. Magi, P. Mirabel and C. George, *J. Phys. Chem. A* 1998, **102**, 593.

3 E. M. Knipping, M. J. Lakin, K. L. Foster, P. Jungwirth, D. J. Tobias, R. B. Gerber, D. Dabdub and B. J. Finlayson-Pitts, *Science* 2000, **288**, 301.

4 S. W. Hunt, M. Roeselová, W. Wang, L. M. Wingen, E. M. Knipping, D. J. Tobias, D. Dabdub and B. J. Finlayson-Pitts, *J. Phys. Chem. A* 2004, **108**, 11559.

5 B. S. Ault, *J. Am. Chem. Soc.* 1978, **100**, 2426.

6 A. Mizoguchi, Y. Ohshima and Y. Endo, *J. Am. Chem. Soc.* 2003, **125**, 1716.

7 D. Liu, G. Ma, L. M. Levering and H. C. Allen, *J. Phys. Chem. B* 2004, **108**, 2252.

8 S. Ghosal, J. C. Hemminger, H. Bluhm, B. S. Mun, E. L. Hebenstreit, G. Ketteler, D. F. Ogletree, F. G. Requejo and M. Salmeron, *Science* 2005, **307**, 563.

9 J. C. H. Sutapa Ghosal, Hendrik Bluhm, Bongjin Simon Mun, Eleonore L. D. Hebenstreit, Guido Ketteler, D. Frank Ogletree, Felix G. Requejo, Miquel Salmeron, *Science* 2005, **307**, 563.

10 D. E. Smith and L. X. Dang, *J. Chem. Phys.* 1994, **100**, 3757.

11 T. Asada and K. Nishimoto, *Chem. Phys. Lett.* 1995, **232**, 518.
12 D. E. Woon and T. H. Dunning, Jr., *J. Am. Chem. Soc.* 1995, **117**, 1090.
13 T. Asada and K. Nishimoto, *Mol. Simul.* 1996, **16**, 307.
14 C. P. Petersen and M. S. Gordon, *J. Phys. Chem. A* 1999, **103**, 4162.
15 P. Jungwirth and D. J. Tobias, *J. Phys. Chem. B* 2000, **104**, 7702.
16 S. Yamabe, H. Kouno and K. Matsumura, *J. Phys. Chem. B* 2000, **104**, 10242.
17 P. Jungwirth and D. J. Tobias, *J. Phys. Chem. B* 2001, **105**, 10468.
18 S. Godinho, P. C. do Couto and B. C. Cabral, *Chem. Phys. Lett.* 2004, **399**, 200.
19 C. Krekeler, B. Hess and L. D. Site, *J. Chem. Phys.* 2006, **125**, 054305.
20 A. C. Olleta, H. M. Lee and K. S. Kim, *J. Chem. Phys.* 2007, **126**, 144311.
21 T. J. Martinez and R. D. Levine, *J. Chem. Phys.* 1996, **105**, 6334.
22 T. J. Martinez and R. D. Levine, *Chem. Phys. Lett.* 1996, **259**, 252.
23 G. H. Peslherbe, B. M. Ladanyi and J. T. Hynes, *J. Phys. Chem. A* 2000, **104**, 4533.
24 D. M. Koch, Q. K. Timerghazin, G. H. Peslherbe, B. M. Ladanyi and J. T. Hynes, *J. Phys. Chem. A* 2006, **110**, 1438.
25 A. C. Olleta, H. M. Lee and K. S. Kim, *J. Chem. Phys.* 2006, **124**, 024321.
26 G. H. Peslherbe, B. M. Ladanyi and J. T. Hynes, *Chem. Phys.* 2000, **258**, 201.
27 G. H. Peslherbe, B. M. Ladanyi and J. T. Hynes, *J. Phys. Chem. A* 1998, **102**, 4100.
28 G. Gregoire, M. Mons, I. Dimicoli, C. Dedonder-Lardeux, C. Jouvet, S. Martrenchard and D. Solgadi, *J. Chem. Phys.* 2000, **112**, 8794.
29 G. Grégoire, M. Mons, C. Dedonder-Lardeux and C. Jouvet, *Eur. Phys. J. D* 1998, **1**, 5.
30 G. Grégoire, M. Mons, I. Dimicoli, F. Piuzzi, E. Charron, C. Dedonder-Lardeux, C. Jouvet, S. Martrenchard, D. Solgadi and A. Suzor-Weiner, *Eur. Phys. J. D* 1998, **1**, 187.
31 E. A. Raymond and G. L. Richmond, *J. Phys. Chem. B* 2004, **108**, 5051.
32 A. T. Blades, M. Peschke, U. H. Verkerk and P. Kebarle, *J. Am. Chem. Soc.* 2004, **126**, 11995.
33 Q. Zhang, C. J. Carpenter, P. R. Kemper and M. T. Bowers, *J. Am. Chem. Soc.* 2003, **125**, 3341.
34 D. E. Woon, *J. Phys. Chem.* 1994, **98**, 8831.
35 C.-W. Liu, G.-L. Hou, W.-J. Zheng and Y. Q. Gao, *Theor. Chem. Acc.* 2014, **133**, 1.
36 D. J. Fatemi and L. A. Bloomfield, *Physical Review A* 2002, **66**, 013202.
37 H.-G. Xu, Z.-G. Zhang, Y. Feng, J. Yuan, Y. Zhao and W. Zheng, *Chem. Phys. Lett.* 2010, **487**, 204.
38 M. J. Frisch et al., *GAUSSIAN 09, Gaussian, Inc., Wallingford, CT,* 2009,
39 O. A. Vydrov and G. E. Scuseria, *J. Chem. Phys.* 2006, **125**, 234109.
40 O. A. Vydrov, J. Heyd, A. V. Krukau and G. E. Scuseria, *J. Chem. Phys.* 2006, **125**, 074106.
41 O. A. Vydrov, G. E. Scuseria and J. P. Perdew, *J. Chem. Phys.* 2007, **126**, 154109.
42 R.-Z. Li, C.-W. Liu, Y. Q. Gao, H. Jiang, H.-G. Xu and W.-J. Zheng, *J. Am. Chem. Soc.* 2013, **135**, 5190.
43 R. Krishnan, J. S. Binkley, R. Seeger and J. A. Pople, *J. Chem. Phys.* 1980, **72**, 650.
44 W. R. Wadt and P. J. Hay, *J. Chem. Phys.* 1985, **82**, 284.
45 K. L. Schuchardt, B. T. Didier, T. Elsethagen, L. Sun, V. Gurumoorthi, J. Chase, J. Li and T. L. Windus, *J. Chem. Inf. Model.* 2007, **47**, 1045.
46 G. D. Purvis and R. J. Bartlett, *J. Chem. Phys.* 1982, **76**, 1910.
47 G. E. Scuseria, C. L. Janssen and H. F. Schaefer, *J. Chem. Phys.* 1988, **89**, 7382.
48 M. Head-Gordon, J. A. Pople and M. J. Frisch, *Chem. Phys. Lett.* 1988, **153**, 503.
49 S. Sæbø and J. Almlöf, *Chem. Phys. Lett.* 1989, **154**, 83.
50 M. J. Frisch, M. Head-Gordon and J. A. Pople, *Chem. Phys. Lett.* 1990, **166**, 275.
51 E. R. Johnson, S. Keinan, P. Mori-Sánchez, J. Contreras-García, A. J. Cohen and W. Yang, *J. Am. Chem. Soc.*

2010, **132**, 6498.

52 T. Lu and F. Chen, *J. Comput. Chem.* 2012, **33**, 580.

53 A. Aguado, A. Ayuela, J. López and J. Alonso, *J. Phys. Chem. B* 1997, **101**, 5944.

54 E. D. Glendening, A. E. Reed, J. E. Carpenter and F. Weinhold, *NBO Version 3.1*

55 A. D. Becke and K. E. Edgecombe, *J. Chem. Phys.* 1990, **92**, 5397.

Table 1 Experimentally observed ADEs and VDEs of $(NaI)_2^-(H_2O)_n$ (n = 0-6) from their photoelectron spectra

isomer	X′		X	
	ADE(eV)	VDE(eV)	ADE(eV)	VDE(eV)
$(NaI)_2^-$			1.56±0.08	1.70±0.08
$(NaI)_2^-(H_2O)$	1.03±0.10	1.24±0.10	1.46±0.08	1.62±0.08
$(NaI)_2^-(H_2O)_2$	0.83±0.10	1.18±0.10	1.37±0.10	1.62±0.08
$(NaI)_2^-(H_2O)_3$	0.74±0.08	1.04±0.10	1.37±0.10	1.59±0.08
$(NaI)_2^-(H_2O)_4$	0.75±0.08	1.00±0.08		
$(NaI)_2^-(H_2O)_5$	0.79±0.08	1.07±0.08		
$(NaI)_2^-(H_2O)_6$	0.84±0.08	1.08±0.08		

Table 2 Relative energies of the low energy isomers of $(NaI)_2(H_2O)_n^-$(n = 0-6) as well as the comparison of their theoretical VDEs to the experiments. The 6-311++G** basis set was used for Na, O and H atoms. The LANL2DZdp ECP basis set was used for iodine atom.

isomer		ΔE* (eV)	Sym.	State	Theo.		Expt.
					VDE (eV)		VDE (eV)
					LC-ωPBE	CCSD(T)	
$(NaI)_2^-$	0A	0.00	C_s	^2A	1.83	1.62	1.70
	0B	0.27	C_{2v}	$^2A_1$	0.80	0.62	
$(NaI)_2(H_2O)^-$	1A	0.00	C_1	^2A	1.77	1.58	1.62
	1B	0.17	C_1	^2A	1.55	1.37	1.24
$(NaI)_2(H_2O)_2^-$	2A	0.00	C_s	^2A	1.85	1.65	1.62
	2B	0.02	C_2	^2A	1.56	1.39	1.18
	2C	0.05	C_1	^2A	1.30	1.13	
$(NaI)_2(H_2O)_3^-$	3A	0.00	C_1	^2A	1.70	1.50	1.59
	3B	0.01	C_1	^2A	1.16	1.04	1.04
	3C	0.04	C_1	^2A	1.26	1.10	
$(NaI)_2(H_2O)_4^-$	4A	0.00	C_s	^2A	1.28	1.16	1.00
	4B	0.08	C_s	^2A	1.19	1.07	
$(NaI)_2(H_2O)_5^-$	5A	0.00	C_1	^2A	1.29		1.07
	5B	0.05	C_1	^2A	1.08		
$(NaI)_2(H_2O)_6^-$	6A	0.00	C_1	^2A	1.25		1.08
	6B	0.02	C_1	^2A	1.08		

* The ΔE values are from the LC-ωPBE functional.

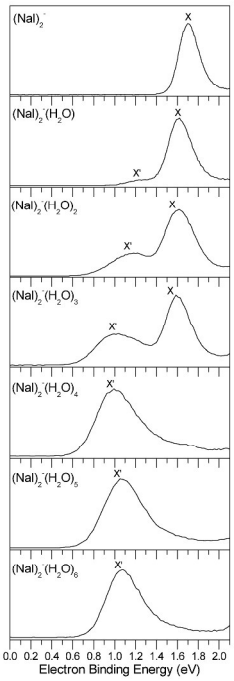

Figure 1. The photoelectron spectra of $(NaI)_2^-(H_2O)_n$ (n = 0-6) clusters measured with 532 nm photons

297x420mm (300 x 300 DPI)

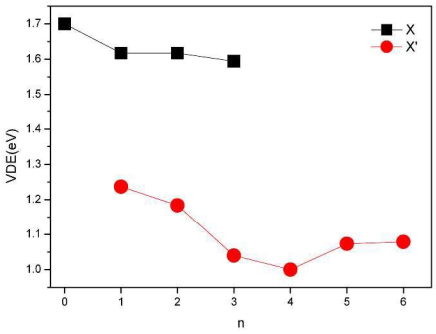

Figure 2. The change of VDEs with the number of water molecules in $(NaI)_2^-(H_2O)_n$ (n = 0-6) clusters.

297x420mm (300 x 300 DPI)

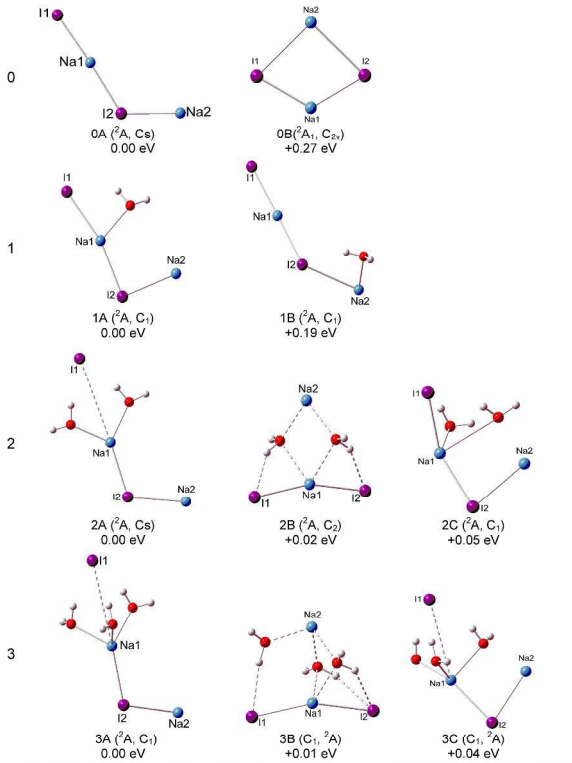

Figure 3. Optimized geometries of the low-lying isomers of $(NaI)_2(H_2O)_n^-$ (n = 0-3) cluster anions.

297x420mm (300 x 300 DPI)

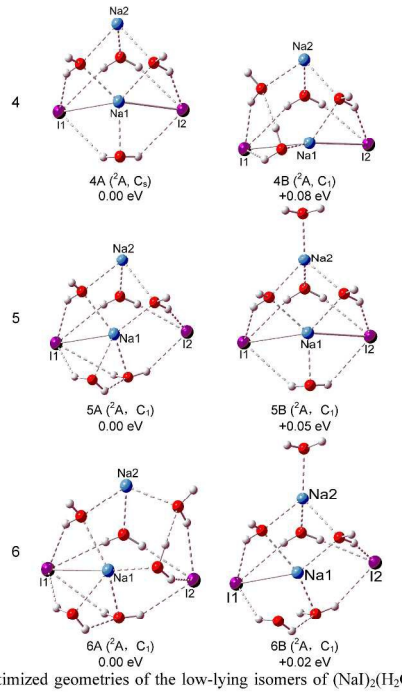

Figure 4. Optimized geometries of the low-lying isomers of $(NaI)_2(H_2O)_n^-$ (n = 4-6) cluster anions.

297x420mm (300 x 300 DPI)

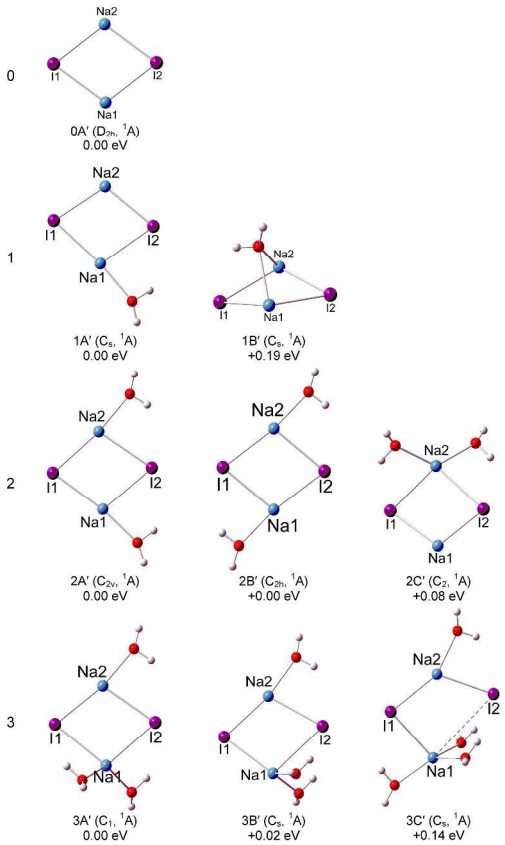

Figure 5. Optimized geometries of the low-lying isomers of neutral $(NaI)_2(H_2O)_n$ (n = 0-3) clusters.

297x420mm (300 x 300 DPI)

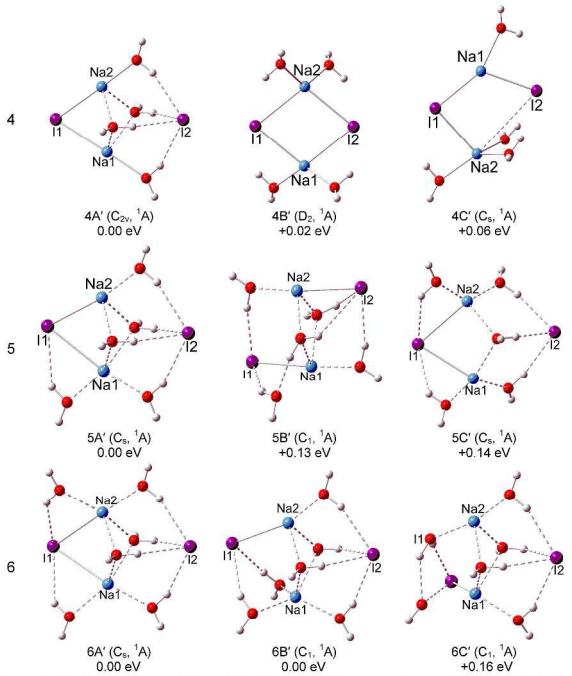

Figure 6. Optimized geometries of the low-lying isomers of neutral $(NaI)_2(H_2O)_n$ (n = 4-6) clusters.

297x420mm (300 x 300 DPI)

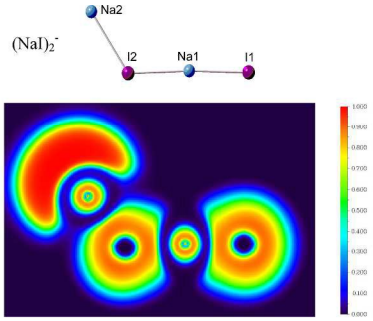

Figure 7. The electron localization function of $(NaI)_2^-$.

297x420mm (300 x 300 DPI)

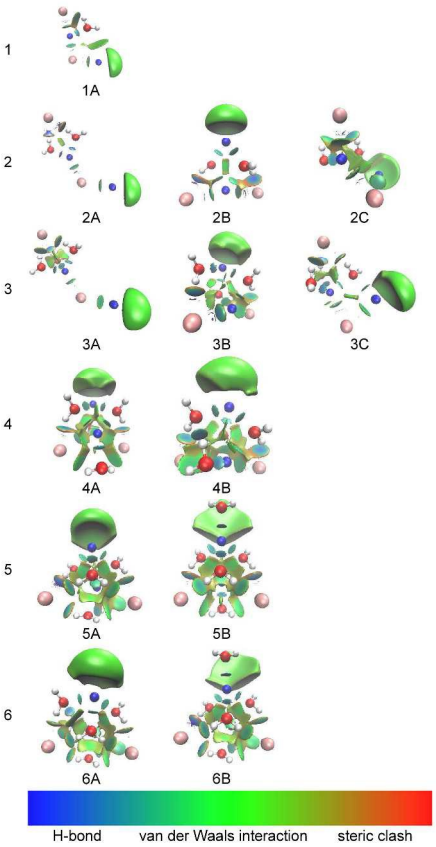

Figure 8. Gradient isosurfaces (s=0.6 au) for $(NaI)_2(H_2O)_n^-$ (n = 1-6) clusters. The surfaces are colored on a blue-green-red scale according to values of sign(λ_2)ρ, ranging from -0.03 to 0.02 au. Blue indicates strong attractive interactions, and red indicates steric clash.

297x420mm (300 x 300 DPI)